

Synthesis, crystal structure and polymorphism of a μ -oxo bridged binuclear iron(III) complex of 2,2':6',2'':6'',2''':6''',2''''-quaterpyridine

Fausto Calderazzo,*[†] Luca Labella and Fabio Marchetti

Dipartimento di Chimica e Chimica Industriale Università di Pisa, via del Risorgimento, 35, I-56126 Pisa, Italy

Aqueous solutions of iron(III) perchlorate and 2,2':6',2'':6'',2''':6''',2''''-quaterpyridine (L, C₂₀H₁₄N₄) in the presence of triethylamine gave deep red crystals of two polymorphic phases of [$\{\text{FeL}(\text{H}_2\text{O})\}_2(\mu\text{-O})\][\text{ClO}_4]_4 \cdot 2\text{H}_2\text{O}$ **1**, a μ -oxo derivative of iron(III). One has been identified as a monoclinic phase, space group $P2_1/n$, with unit cell $a = 13.080(3)$, $b = 14.045(3)$, $c = 13.778(3)$ Å, $\beta = 105.52(3)^\circ$ and the other as an orthorhombic one, space group $Pbca$ with unit cell $a = 14.175(2)$, $b = 16.463(1)$ and $c = 20.949(3)$ Å. The crystal structures of both polymorphs have been studied and shown to correspond to slightly different geometries of the same cation. To reduce some degree of disorder in the perchlorate anions, the monoclinic phase has also been studied at -150°C , giving an ordered pattern. The crystal structures of the two phases are compared. The two iron atoms are at the centre of corner-sharing octahedra, with the water *trans* to the μ -bonded oxide.

Binuclear complexes containing a μ -oxo diiron core, which were reviewed in 1990,¹ are currently studied as models for non-heme oxoiron proteins.² While μ -(oxo)iron(III) complexes are numerous and well characterised, μ -(oxo)iron(II) derivatives are rare. The pentaoxodiiron(II) anion [Fe_2O_5]⁶⁻ was obtained by a high-temperature reduction of the oxoiron(III) precursor on the wall of an iron cylinder.³ Recently, some of us have reported the uncharged μ -(oxo)iron(II) compound, [$\text{Fe}_8(\mu\text{-O})_2(\text{O}_2\text{CNPt}^{\text{I}})_2$]₁₂, which was obtained by controlled hydrolysis of [$\text{Fe}(\text{O}_2\text{CN-Pr}^{\text{I}})_2$]_n under anaerobic conditions.⁴ In addition, Lippard and co-workers have isolated and crystallographically established several examples of μ -oxo derivatives containing both iron(II) and iron(III) in the same chemical entity.⁵ In view of the elusive character of μ -oxo derivatives of iron(II), our interest was attracted by a paper describing the synthesis of the binuclear μ -oxo bridged iron(II) quaterpyridine complex [$\{\text{FeL}(\text{ClO}_4)\}_2(\mu\text{-O})\cdot 8.5\text{H}_2\text{O}$, reported to be synthesised from iron(III) perchlorate in aqueous solution; exclusion of air was not specifically indicated.⁶ The presence of iron(II) under these conditions appeared to be rather intriguing; in fact, although the reduction potential of iron(III) to iron(II) in the presence of quaterpyridine at pH 3 is +0.58 V,⁷ binuclear μ -oxo bridged iron(III) quaterpyridine sulfate complexes have been prepared by Pispisa and co-workers starting from aqueous iron(II) sulfate with an alcoholic solution of quaterpyridine.^{8a} Equally unusual is the fact that the perchlorate anion is a ligand for iron in preference to water. Among the hydrated perchlorate complexes crystallographically studied and in which both H₂O and ClO₄⁻ have some kind of interaction with the metal centre,^{8b-d} only one definitely displays a metal co-ordinated perchlorate ligand in a rather special arrangement within a cage of 18 metal atoms.^{8d} We therefore decided to reinvestigate the system reported by Che *et al.*⁶ It is the purpose of this paper to report that we found no evidence of the iron(II) μ -oxo complex. Our own work led to the isolation of a new μ -oxo derivative of iron(III) and to the identification of two polymorphs containing the same μ -oxo cation of iron(III), [$\text{Fe}_2(\mu\text{-O})\text{L}_2(\text{H}_2\text{O})_2$]⁴⁺.

Experimental

2,2':6',2'':6'',2''':6''',2''''-Quaterpyridine (L) was prepared according to a literature method.⁹ The compound Fe(ClO₄)₃·H₂O was

purchased from Aldrich and used as received. All reactions were carried out under exclusion of air. Infrared spectra were measured with a Perkin-Elmer FT-IR 1725 X instrument. Magnetic susceptibility data were obtained with a Faraday balance, calibrated with CuSO₄·5H₂O. Elemental analyses (C, H, N) were performed by Laboratorio di Microanalisi della Facoltà di Farmacia, Università di Pisa, with a Carlo Erba model 1106 elemental analyser.

Synthesis of [$\{\text{FeL}(\text{H}_2\text{O})\}_2(\mu\text{-O})\][\text{ClO}_4]_4 \cdot 2\text{H}_2\text{O}$ **1**

Method (a). An aqueous solution (20 cm³) of iron(III) perchlorate, Fe(ClO₄)₃·H₂O (0.20 g, 0.54 mmol) was treated with 2,2':6',2'':6'',2''':6''',2''''-quaterpyridine (0.17 g, 0.54 mmol) and NEt₃ (0.075 ml, 0.54 mmol) in a closed vessel at 140 °C for 5 h. When the solution was cooled over a period of 8 h, red crystals were obtained (0.25 g, 75% yield). The solid crystalline product turned out to be quite stable in air. The compound analysed correctly for [$\{\text{FeL}(\text{H}_2\text{O})\}_2(\mu\text{-O})\][\text{ClO}_4]_4 \cdot 2\text{H}_2\text{O}$ (Found: C, 39.5; H, 3.1; N, 9.1. C₄₀H₃₆Cl₄Fe₂N₈O₂₁ requires C, 39.4; H, 3.0; N, 9.2%). IR Nujol (1800–400 cm⁻¹): 1620m, 1603s, 1584w, 1575w, 1566w, 1530m, 1495m, 1470s, 1445m, 1399w, 1378m, 1319m, 1296m, 1269m, 1253m, 1227w, 1199w, 1146s, 1099vs (br), 1024m, 992w, 942w, 932w, 835s ($\mu\text{-O}$), 820s (sh), 779s, 736w, 713w, 659m, 637 (sh), 627s, 579w, 437w. The magnetic susceptibility of the product is $\chi_{\text{Fe}}^{\text{corr}} = 1141 \times 10^{-6}$ cgsu (diamagnetic correction = -303×10^{-6} cgsu), corresponding to $\mu_{\text{eff}} = 1.63 \mu_{\text{B}}$ ($\approx 1.51 \times 10^{-23}$ J T⁻¹) at 290 K. Magnetic susceptibilities in the temperature range between 80 and 290 K are satisfactorily fit by the conventional spin–spin interaction model,¹⁰ assuming spin $\frac{5}{2}$ for both nuclei and no temperature-independent paramagnetic contribution. Fitting parameters: $g = 1.76(6)$ and $J = -94(5)$ cm⁻¹.

Method (b). An aqueous solution (18 cm³) of iron(III) perchlorate, Fe(ClO₄)₃·H₂O (0.20 g, 0.54 mmol) was treated with 2,2':6',2'':6'',2''':6''',2''''-quaterpyridine (0.05 g, 0.16 mmol) and EtOH (2 cm³). The slightly soluble quaterpyridine reacted slowly. The orange-red precipitate was filtered after 1 d stirring (0.05 g, 50% yield with respect to quaterpyridine). An IR spectrum was superimposable on that of compound **1** prepared by method (a). Heating this solid in the original solvent mixture produced a dark red solution which was cooled over a period of 8 h, producing red crystals. One of the single crystals selected for an X-ray diffractometric experiment showed the

[†] E-Mail: facal@dccu.unipi.it

Table 1 Crystal data and structure refinement for **1m**, **1m IT**, **1o**

Sample	1m	1m IT	1o
Empirical formula	C ₄₀ H ₃₆ Cl ₄ Fe ₂ N ₈ O ₂₁	C ₄₀ H ₃₆ Cl ₄ Fe ₂ N ₈ O ₂₁	C ₄₀ H ₃₆ Cl ₄ Fe ₂ N ₈ O ₂₁
<i>M</i>	1218.27	1218.27	1218.27
<i>T</i> /K	293(2)	143(1)	293(2)
$\lambda/\text{\AA}$	0.710 73	0.710 73	0.710 73
Crystal system	Monoclinic	Monoclinic	Orthorhombic
Space group	<i>P</i> 2 ₁ / <i>n</i> (no. 14)	<i>P</i> 2 ₁ / <i>n</i> (no. 14)	<i>Pbca</i> (no. 61)
<i>a</i> / \AA	13.080(3)	12.912(2)	14.175(2)
<i>b</i> / \AA	14.045(3)	13.913(4)	16.463(1)
<i>c</i> / \AA	13.778(3)	13.545(2)	20.949(3)
$\beta/^\circ$	105.52(3)	105.36(1)	—
<i>U</i> / \AA^3	2438.8(8)	2346.4(8)	4888.7(10)
<i>Z</i>	2	2	4
<i>D_c</i> /Mg m ³	1.659	1.724	1.655
μ/mm^{-1}	0.903	0.939	0.901
<i>F</i> (000)	1240	1240	2480
Crystal size/mm	0.31 × 0.20 × 0.14	0.31 × 0.20 × 0.14	0.44 × 0.32 × 0.12
θ Range for data collection ^o	1.91 to 21.25	2.14 to 25.00	2.13 to 22.50
Index ranges	−1 ≤ <i>h</i> ≤ 13, −1 ≤ <i>k</i> ≤ 14, −14 ≤ <i>l</i> ≤ 13	−1 ≤ <i>h</i> ≤ 15, −1 ≤ <i>k</i> ≤ 16, −16 ≤ <i>l</i> ≤ 15	−1 ≤ <i>h</i> ≤ 14, −1 ≤ <i>k</i> ≤ 17, −1 ≤ <i>l</i> ≤ 22
Reflections collected	3472	5145	3995
Independent reflections [<i>R</i> _{int}]	2703 [0.0403]	4129 [0.0522]	3189 [0.0326]
Refinement method	Full-matrix least-squares on <i>F</i> ²	Full-matrix least-squares on <i>F</i> ²	Full-matrix least-squares on <i>F</i> ²
Data, restraints, parameters	2702, 6, 320	4129, 0, 356	3189, 0, 297
Goodness of fit ^a on <i>F</i> ²	1.049	1.034	1.010
Final <i>R</i> indices ^a [<i>I</i> > 2σ(<i>I</i>): <i>R</i> ₁ , <i>wR</i> ₂	0.0868, 0.2260	0.0634, 0.1166	0.1069, 0.2976
<i>R</i> indices (all data) ^a : <i>R</i> ₁ , <i>wR</i> ₂	0.1383, 0.2740	0.1263, 0.1436	0.1770, 0.3759
Largest difference peak, hole/e \AA^{-3}	1.683, −0.683	0.541, −0.502	1.199, −0.609
<i>A</i> , <i>B</i> (<i>w</i>) ^a	0.1440, 14.02	0.0469, 2.42	0.2489, 4.97

^a $R_1 = \Sigma||F_o| - |F_c||/\Sigma|F_o|$; $wR_2 = \{\Sigma[w(F_o^2 - F_c^2)^2]/\Sigma[w(F_o^2)^2]\}^{1/2}$; $w = 1/[\sigma^2(F_o^2) + (AQ)^2 + BQ]$ where $Q = [\max(F_o^2, 0) + 2F_c^2]/3$, goodness of fit = $[\Sigma(w(F_o^2 - F_c^2)^2)/(N - P)]^{1/2}$, where *N*, *P* are the numbers of observations and parameters, respectively.

monoclinic cell *a* = 13.08(1), *b* = 14.025(3), *c* = 13.752(8) \AA , β = 105.48(7) $^\circ$.

Crystallography

Structure determination of the monoclinic phase 1m. (*a*) *At room temperature.* A dark red crystal of **1m**, obtained from an aqueous solution as previously described, was glued at the end of a glass fibre and mounted on a Siemens P4 automatic single-crystal X-ray diffractometer equipped with graphite-monochromatized Mo-K α radiation ($\lambda = 0.7107 \text{ \AA}$), obtaining the crystal parameters listed in Table 1. The cell parameters were obtained from the setting angles of 17 accurately centred strong reflections having θ between 8.4 and 10.1 $^\circ$. A redundant set of intensities was collected by testing the crystal stability and alignment with three standard reflections monitored every 97 measurements. The intensities were corrected for Lorentz and polarisation effects and for absorption by using a ψ -scan method.¹¹ The internal reliability factor $R_{\text{int}} = \Sigma|F_o^2 - F_o^2(\text{mean})|/\Sigma|F_o^2|$ after the corrections, calculated on the equivalent reflections, is given in Table 1. The space group was unequivocally established on the basis of systematic extinctions and the structure was solved by using the automatic direct methods of the SIR 92 program.¹² The thermal parameters of the perchlorate oxygen atoms showed a tendency to increase during the refinement. Those of the central chlorine atoms were instead nearly normal; this has been attributed to an orientational disorder that leaves the position of the centroids unchanged. An attempt to refine the structure by imposing an ideal geometry to the anions gave unsatisfactory *R* factors. The refinement was therefore continued without geometrical constraints, thus obtaining the final reliability factors listed in Table 1. The refinement has been carried out using the SHELXTL program.¹³

(*b*) *At low temperature.* Since the structure of $[\{\text{FeL}(\text{H}_2\text{O})\}_2(\mu\text{-O})][\text{ClO}_4]_4 \cdot 2\text{H}_2\text{O}$ showed non-bonding O...O distances between the water molecules and the perchlorate anions shorter than the sum of the van der Waals radii, thus suggesting

strong hydrogen-bond interactions, we decided to carry out a diffractometric experiment at low temperature (−130 $^\circ\text{C}$) on the same crystal in an attempt to reach a more accurate determination of the bonding parameters.

The crystal of the monoclinic phase was mounted on the same diffractometer, equipped with a Siemens LT-2A low-temperature device, and the intensity data were collected under the conditions summarised in Table 1, entry **1m IT**. The collected data were treated as in the previous case and the final atomic positions obtained at room temperature were refined with the new data set. The oxygen atoms now presented normal thermal parameters, the perchlorate anions showing the usual tetrahedral geometry and all the hydrogen atoms were located on the Fourier-difference map. The final reliability factors are listed in Table 1.

Structure determination of the orthorhombic phase 1o. A dark red crystal of $[\{\text{FeL}(\text{H}_2\text{O})\}_2(\mu\text{-O})][\text{ClO}_4]_4 \cdot 2\text{H}_2\text{O}$, obtained from aqueous solution was glued at the end of a glass fibre and mounted on the Siemens P4 automatic single-crystal X-ray diffractometer. The unit cell parameters listed in the last column of Table 1 have been obtained from the setting angles of 14 accurately centred strong reflections having θ between 10.5 and 12.3 $^\circ$. The intensity data were collected following the conditions listed in Table 1 and were corrected for Lorentz, polarisation and absorption with the ψ -scan method. After correction, the equivalent reflections were merged giving an R_{int} of 0.0326. The structure was solved by direct methods and the following Fourier maps showed the positions of all the heavy atoms. Quaterpyridine hydrogen atoms were introduced in calculated positions and water hydrogens have been omitted. The final refinement cycle was made with isotropic thermal parameters for hydrogen atoms and for perchlorate oxygen atoms and anisotropic for the others. The final reliability factors are listed in Table 1.

CCDC reference number 186/925.

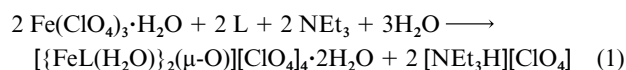
See <http://www.rsc.org/suppdata/dt/1998/1485/> for crystallographic files in .cif format.

Powder diffraction measurements

Product **1** was milled in a mortar and was spread on a quartz plate and its X-ray powder diffraction pattern was recorded with a Philips PW1050/25 Bragg–Brentano diffractometer, using Ni-filtered Cu-K α radiation ($\lambda = 1.54178 \text{ \AA}$). The recorded pattern was then compared with those calculated¹⁴ from the single crystal data of **1m**, **1o** and $[\{\text{FeL}(\text{ClO}_4)\}_2(\mu\text{-O})] \cdot 8.5\text{H}_2\text{O}$.⁶ All of the more intense lines of the calculated pattern of **1m** together with some of the lines calculated for **1o** were present in the diffraction pattern of the specimen, with **1m** largely prevailing. None of the lines expected for $[\{\text{FeL}(\text{ClO}_4)\}_2(\mu\text{-O})] \cdot 8.5\text{H}_2\text{O}$ was detected: particularly, the intense peak at $d 14.025 \text{ \AA}$ was absent.

Results and Discussion

A hydrothermal synthesis of $[\{\text{FeL}(\text{H}_2\text{O})\}_2(\mu\text{-O})][\text{ClO}_4]_4 \cdot 2\text{H}_2\text{O}$ was carried out in a closed vessel, under a dinitrogen atmosphere, according to the stoichiometry of equation (1). The



acidity of the iron-co-ordinated water favours deprotonation.^{15a} In water the hexaaqua complex of iron(III) perchlorate predominates only at pH about 0; at higher pH, hydrolysis occurs.^{15b} Multidentate bulky ligands, such as 2,2':6',2'':6'',2'''-quaterpyridine (L), can stabilise the system towards further hydrolysis. In the synthesis, triethylamine was added in order to neutralise the acidity liberated in the reaction. The reaction by-product, $[\text{NEt}_3\text{H}][\text{ClO}_4]$, is soluble in cold water, while the iron complex, $[\{\text{FeL}(\text{H}_2\text{O})\}_2(\mu\text{-O})][\text{ClO}_4]_4 \cdot 2\text{H}_2\text{O}$ has a low solubility at room temperature, thus facilitating its recovery. The compound is characterised by an IR band at 835 cm^{-1} which is attributed to the asymmetric vibration of the Fe–O–Fe system.^{8a}

Red crystals of two different types, both corresponding to the same compound, $[\{\text{FeL}(\text{H}_2\text{O})\}_2(\mu\text{-O})][\text{ClO}_4]_4 \cdot 2\text{H}_2\text{O}$ were obtained. One of the two polymorphs is monoclinic with a cell volume of 2439 \AA^3 , while the other is orthorhombic with a primitive cell whose volume is 4889 \AA^3 . We will refer to them as **1m** for the monoclinic phase and **1o** for the orthorhombic one. At room temperature, both phases are disordered in the orientation of the perchlorate groups, which prevented an accurate location of the oxygen atoms. In order to reduce the disorder, the diffractometric experiment on the monoclinic crystal was carried out also at 143 K (we shall refer to that measurement as **1m IT**). The molecular structure is practically the same in both phases and we shall describe only the results which are not affected by the disorder of the anions and show the lowest standard deviations. Later on, the crystal structures will be compared.

The molecular structure of the $[\{\text{FeL}(\text{H}_2\text{O})\}_2(\mu\text{-O})]^{4+}$ cation is shown in Fig. 1, bond distances and angles being listed in Table 2. The iron is octahedrally co-ordinated to two oxygen atoms and to four nitrogens of the quaterpyridine ligand. The geometry of the chelating ligand forces it to occupy four in-plane co-ordinative positions. The $\mu\text{-O}$ –Fe and O(W1)–Fe distances of 1.776(1) and 2.063(5) \AA , respectively, are in keeping with the mean values of 1.79(6) and 2.09(7) \AA reported¹⁶ for such bond distances in iron(III) complexes at room temperature. The Fe–N bond distances from the nitrogen atoms of the internal rings show a mean value of 2.116 \AA , significantly shorter than the mean value of 2.192 \AA observed for the terminal rings. Both values, however, compare well with the value of 2.22(10) \AA calculated¹⁶ as the mean of the Fe–N bond lengths in fourteen iron–pyridine complexes. The Fe–N bond length difference between the internal and terminal nitrogens is probably due to the strain induced by quaterpyridine,

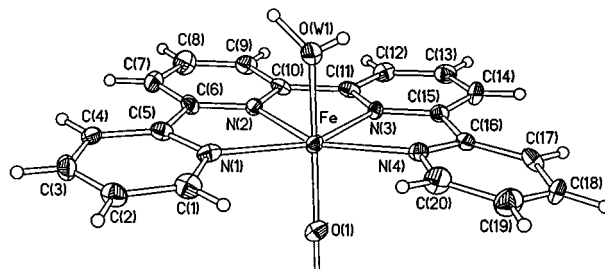


Fig. 1 Cationic moiety of the asymmetric unit in the structure of monoclinic phase of **1** at $T = 143 \text{ K}$ (**1m**, **IT**). Thermal ellipsoids are at 50% probability

Table 2 Bond lengths (\AA) and angles ($^\circ$) for compound **1m IT**

Fe–O(1)	1.776(1)	C(7)–C(8)	1.380(9)
Fe–O(W1)	2.063(5)	C(8)–C(9)	1.38(1)
Fe–N(3)	2.115(5)	C(9)–C(10)	1.392(8)
Fe–N(2)	2.118(5)	C(10)–C(11)	1.496(9)
Fe–N(4)	2.191(5)	C(11)–C(12)	1.387(9)
Fe–N(1)	2.194(6)	C(12)–C(13)	1.38(1)
O(1)–Fe'	1.776(1)	C(13)–C(14)	1.374(9)
N(1)–C(5)	1.342(8)	C(14)–C(15)	1.394(8)
N(1)–C(1)	1.351(8)	C(15)–C(16)	1.480(8)
N(2)–C(10)	1.338(7)	C(16)–C(17)	1.379(9)
N(2)–C(6)	1.347(8)	C(17)–C(18)	1.387(9)
N(3)–C(11)	1.344(7)	C(18)–C(19)	1.380(9)
N(3)–C(15)	1.348(8)	C(19)–C(20)	1.38(1)
N(4)–C(20)	1.343(8)	Cl(1)–O(5)	1.426(5)
N(4)–C(16)	1.356(8)	Cl(1)–O(3)	1.432(4)
C(1)–C(2)	1.38(1)	Cl(1)–O(4)	1.437(5)
C(2)–C(3)	1.38(1)	Cl(1)–O(2)	1.443(5)
C(3)–C(4)	1.384(9)	Cl(2)–O(9)	1.434(5)
C(4)–C(5)	1.399(9)	Cl(2)–O(7)	1.438(5)
C(5)–C(6)	1.484(8)	Cl(2)–O(8)	1.447(6)
C(6)–C(7)	1.389(9)	Cl(2)–O(6)	1.447(5)
O(1)–Fe–O(W1)	154.6(2)	N(2)–C(6)–C(5)	114.5(6)
O(1)–Fe–N(3)	103.0(2)	C(7)–C(6)–C(5)	124.8(6)
O(W1)–Fe–N(3)	97.1(2)	C(8)–C(7)–C(6)	118.7(6)
O(1)–Fe–N(2)	106.9(2)	C(7)–C(8)–C(9)	120.6(6)
O(W1)–Fe–N(2)	93.4(2)	C(8)–C(9)–C(10)	117.9(6)
N(3)–Fe–N(2)	74.0(2)	N(2)–C(10)–C(9)	121.4(6)
O(1)–Fe–N(4)	87.2(1)	N(2)–C(10)–C(11)	113.4(5)
O(W1)–Fe–N(4)	83.5(2)	C(9)–C(10)–C(11)	125.1(5)
N(3)–Fe–N(4)	74.2(2)	N(3)–C(11)–C(12)	121.7(6)
N(2)–Fe–N(4)	147.4(2)	N(3)–C(11)–C(10)	112.9(5)
O(1)–Fe–N(1)	89.1(1)	C(12)–C(11)–C(10)	125.4(6)
O(W1)–Fe–N(1)	81.8(2)	C(13)–C(12)–C(11)	117.5(6)
N(3)–Fe–N(1)	148.0(2)	C(14)–C(13)–C(12)	121.5(6)
N(2)–Fe–N(1)	74.1(2)	C(13)–C(14)–C(15)	118.0(6)
N(4)–Fe–N(1)	136.6(2)	N(3)–C(15)–C(14)	120.9(6)
Fe–O(1)–Fe'	180.0	N(3)–C(15)–C(16)	113.9(5)
C(5)–N(1)–C(1)	119.0(6)	C(14)–C(15)–C(16)	125.1(6)
C(5)–N(1)–Fe	117.1(4)	N(4)–C(16)–C(17)	120.6(6)
C(1)–N(1)–Fe	123.7(5)	N(4)–C(16)–C(15)	114.6(5)
C(10)–N(2)–C(6)	120.7(5)	C(17)–C(16)–C(15)	124.8(6)
C(10)–N(2)–Fe	119.7(4)	C(16)–C(17)–C(18)	119.9(6)
C(6)–N(2)–Fe	119.6(4)	C(19)–C(18)–C(17)	119.2(6)
C(11)–N(3)–C(15)	120.3(5)	C(18)–C(19)–C(20)	118.6(6)
C(11)–N(3)–Fe	119.8(4)	N(4)–C(20)–C(19)	122.1(6)
C(15)–N(3)–Fe	119.9(4)	O(5)–Cl(1)–O(3)	110.6(3)
C(20)–N(4)–C(16)	119.5(6)	O(5)–Cl(1)–O(4)	108.3(3)
C(20)–N(4)–Fe	123.1(4)	O(3)–Cl(1)–O(4)	110.1(3)
C(16)–N(4)–Fe	116.0(4)	O(5)–Cl(1)–O(2)	109.4(4)
N(1)–C(1)–C(2)	121.8(6)	O(3)–Cl(1)–O(2)	109.4(3)
C(3)–C(2)–C(1)	119.1(6)	O(4)–Cl(1)–O(2)	109.0(4)
C(2)–C(3)–C(4)	119.7(6)	O(9)–Cl(2)–O(7)	109.1(3)
C(3)–C(4)–C(5)	118.4(6)	O(9)–Cl(2)–O(8)	110.0(4)
N(1)–C(5)–C(4)	121.8(6)	O(7)–Cl(2)–O(8)	109.7(4)
N(1)–C(5)–C(6)	114.5(6)	O(9)–Cl(2)–O(6)	109.8(3)
C(4)–C(5)–C(6)	123.6(6)	O(7)–Cl(2)–O(6)	109.6(3)
N(2)–C(6)–C(7)	120.7(6)	O(8)–Cl(2)–O(6)	108.6(3)

Symmetry transformations used to generate equivalent atoms: $' = 2 - x, 1 - y, 1 - z$.

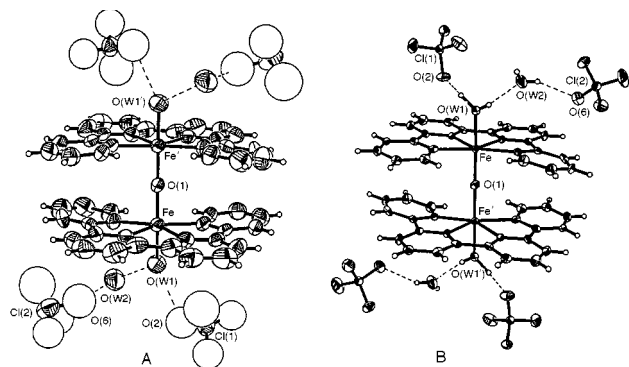


Fig. 2 Hydrogen bonding in the crystal structure of **1**. A: orthorhombic phase at room temperature (**1o**); B: monoclinic phase at 143 K (**1m, IT**)

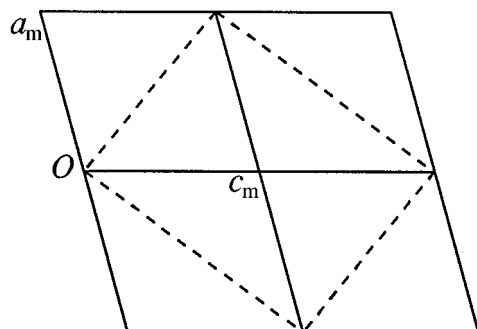


Fig. 3 Pseudo-orthorhombic unit cell (dashed lines) as it can be related to the monoclinic cell of **1** (full lines)

with respect to the ideal octahedral positions. The considerable difference between the N–Fe–N angles of the diazaferracyclopentane rings (mean value 74.1°) and the N(1)–Fe–N(4) angle of 136.6° supports this interpretation.

In both monoclinic and orthorhombic phases the μ -oxo atom lies on an inversion centre, the Fe–O–Fe' angle being 180° by symmetry. Thus, the cation consists of two aqua-iron-quaterpyridine moieties joined by the central oxygen with the chelating ligand on opposite sides. The structure of the compound is completed, for each iron atom, by a water molecule and two perchlorate anions, the latter showing the usual tetrahedral geometry.

The two hydrogen atoms of the water ligand are involved in strong hydrogen bonding with the oxygen atom O(2) [O(W1) \cdots O(2) 2.828 Å] of a perchlorate anion and with the O(W2) oxygen of the second water molecule [O(W1) \cdots O(W2) 2.598 Å]. This water is engaged through one of its hydrogen atoms in a further hydrogen bond with the oxygen O(6) [O(W2) \cdots O(6) 2.796 Å] of the second perchlorate anion, while the other hydrogen atom interacts more weakly with the oxygen O(5'') [O(W2) \cdots O(5'') 3.084 Å] of the nearest perchlorate anion. The apex '' indicates the operation $2 - x, -y, 1 - z$. The presence of this gap in the sequence of hydrogen interactions allows us to consider the crystal structure of compound **1** as being built by units consisting of the $[\{\text{FeL}(\text{H}_2\text{O})\}_2(\mu\text{-O})]^{4+}$ cation, two water molecules and four ClO_4^- anions connected as shown in Fig. 2B. Apart from some minor differences in the metrical data and some orientational disorder in the anions, the building units of the orthorhombic phase are the same. One of them is shown in Fig. 2A.

The monoclinic primitive lattice of **1** can be obtained by means of a pseudo-orthorhombic A-centred cell with $a = 14.045$, $b = 16.263$, $c = 21.386$ Å; $\alpha = 90$, $\beta = 90$, $\gamma = 93.09^\circ$, as indicated in Fig. 3. This cell, having a volume of 4878 Å³, is metrically very similar to that obtained for the orthorhombic phase (see Table 1). A close similarity exists also for some symmetry operations, that are common to the monoclinic $P2_1/n$

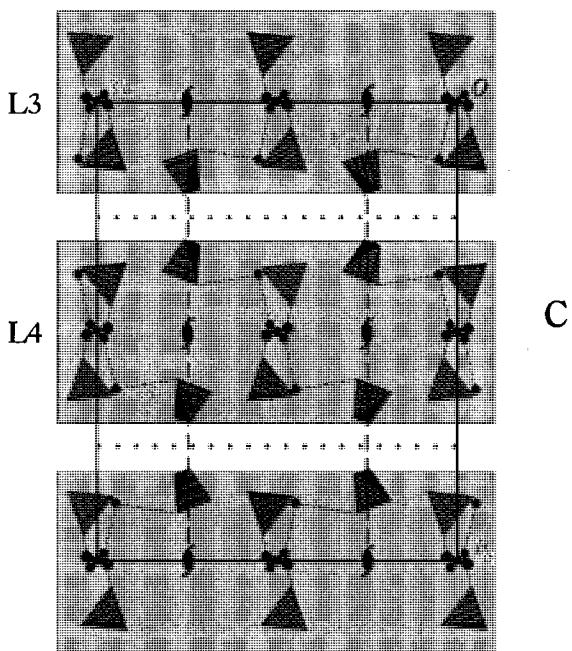
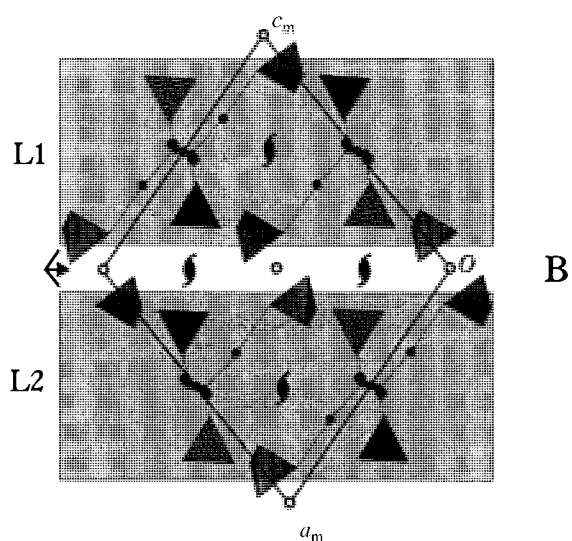
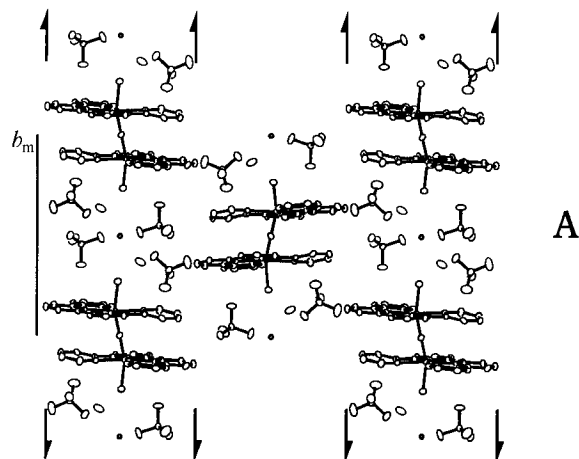


Fig. 4 A: view of a molecular layer in the monoclinic (1 0 1) plane. One half of the inversion centres are occupied by the O(1) atoms. B: layout of layers in the monoclinic phase ($P2_1/n$) viewed in the b direction. The quaterpyridine ligands have been omitted for clarity and substituted by shaded areas. C: layout of layers in the orthorhombic phase ($Pbca$) viewed along the a direction. The structure has been simplified as in B. Only the symmetry operators useful for the discussion in the text have been indicated

cell and to the orthorhombic one, *Pbca*. Thus, the structures of the two phases are closely related and it may be suggested that they can interconvert through a topotactic transformation.¹⁷

Fig. 4A shows a layer of molecules as in the (1 0 1) plane of the monoclinic phase. In them, infinite rows of $[\{\text{FeL}(\text{H}_2\text{O})\}_2(\mu\text{-O})][\text{ClO}_4]_4 \cdot 2\text{H}_2\text{O}$ units are spaced by *b*, the anionic moieties facing each other. Adjacent rows in the layer are shifted by *b*/2, being related by a 2₁ axis parallel to *b*. Along the rows, a series of inversion centres spanned by *b*/2 are also present. Similar, although not exactly identical, layers occur in the (0 1 0) plane of the orthorhombic phase. They are characterised by the same sequence of inversion centres and screw axes.

Fig. 4B shows a schematic layout of layers along the monoclinic *b* direction. The L1 and L2 layers are related by a sequence of screw axes and inversion centres regularly spanned by $a_m/4 + c_m/4$. Fig. 4C displays the same layout in the orthorhombic phase and shows how the layers L3 and L4 are related by a glide with a translation component of $a_o/2$.

Magnetic measurements in the solid state at 290 K show the iron product to be paramagnetic, though the magnetic moment is reduced by antiferromagnetic coupling of the two iron centres. The magnetic data for $[\{\text{FeL}(\text{H}_2\text{O})\}_2(\mu\text{-O})][\text{ClO}_4]_4 \cdot 2\text{H}_2\text{O}$ are in agreement with those reported by Pispisa and co-workers for the iron(III) species $[\{\text{FeL}\}_2(\mu\text{-O})][\text{SO}_4]_2 \cdot 7\text{H}_2\text{O}$.^{8a}

Both crystallographic and magnetic data confirm that $[\{\text{FeL}(\text{H}_2\text{O})\}_2(\mu\text{-O})][\text{ClO}_4]_4 \cdot 2\text{H}_2\text{O}$ is an iron(III) product and that quaterpyridine does not promote reduction of iron(III) perchlorate. In our hands, even in the presence of ethanol, strictly reproducing the conditions and stoichiometry reported⁶ for the iron(II) derivative $[\{\text{FeL}(\text{ClO}_4)\}_2(\mu\text{-O})] \cdot 8.5\text{H}_2\text{O}$, only the iron(III) derivative $[\{\text{FeL}(\text{H}_2\text{O})\}_2(\mu\text{-O})][\text{ClO}_4]_4 \cdot 2\text{H}_2\text{O}$ could be isolated and characterized by X-ray diffraction. The product reported by Che *et al.*⁶ (magnetic susceptibility by the Evans method) has been claimed to contain diamagnetic iron(II). However, no reduction occurs in the synthesis by Pispisa and co-workers,⁸ where, on the contrary, oxidation of aqueous iron(II) sulfate by dioxygen in the presence of the ligand has been reported in ethanol solution.

Conclusion

Although the synthesis⁶ of $[\{\text{FeL}(\text{ClO}_4)\}_2(\mu\text{-O})] \cdot 8.5\text{H}_2\text{O}$ could not be reproduced, the cationic iron(III) core $[\{\text{FeL}\}_2(\mu\text{-O})]^{4+}$ is quite easily obtained and the paramagnetic iron(III) product $[\{\text{FeL}(\text{H}_2\text{O})\}_2(\mu\text{-O})][\text{ClO}_4]_4 \cdot 2\text{H}_2\text{O}$ has been isolated in two different crystalline phases. Since the experimental conditions reported in the earlier paper⁶ did not allow the isolation of any iron(II) μ -oxo derivative, attempts are now being made to identify the conditions under which such a compound can be isolated, possibly starting from perchlorate or sulfate complexes of iron(II).

Acknowledgements

The authors wish to thank the Ministero della Pubblica Istruzione, MURST, for financial support. Drs. Roberto Ambrosetti and Rino Pinzino of Istituto per la Chimica Quantistica ed Energetica Molecolare, ICQEM, CNR, Pisa are gratefully acknowledged for providing the program for computing the magnetic susceptibility.

References

- 1 D. M. Kurtz, jun., *Chem. Rev.*, 1990, **90**, 585.
- 2 S. J. Lippard, *Angew. Chem., Int. Ed. Engl.*, 1988, **27**, 344; L. Que, jun. and A. E. True, *Prog. Inorg. Chem.*, 1990, **38**, 97; J. B. Vincent, G. L. Olivier-Lilley and B. A. Averill, *Chem. Rev.*, 1990, **90**, 1447; A. L. Feig and S. J. Lippard, *Chem. Rev.*, 1994, **94**, 759; E. C. Constable, *Adv. Inorg. Chem. Radiochem.*, 1986, **30**, 69.
- 3 H. P. Müller and R. Hoppe, *Z. Anorg. Allg. Chem.*, 1989, **569**, 16; 1993, **619**, 193.
- 4 D. Belli Dell' Amico, F. Calderazzo, L. Labella, C. Maichle-Mössner and J. Strähle, *J. Chem. Soc., Chem. Commun.*, 1994, 1555.
- 5 K. L. Taft, G. C. Papaefthymiou and S. J. Lippard, *Inorg. Chem.*, 1994, **33**, 1510; W. Micklitz, V. McKee, R. L. Rardin, L. E. Pence, G. C. Papaefthymiou, S. G. Bott and S. J. Lippard, *J. Am. Chem. Soc.*, 1994, **116**, 8061.
- 6 C. M. Che, C. W. Chan, S. M. Yang, C. X. Guo, C. Y. Lee and S. M. Peng, *J. Chem. Soc., Dalton Trans.*, 1995, 2961.
- 7 A. Bergh, P. O'D. Offenhartz, P. George and G. P. Haight, jun., *J. Chem. Soc.*, 1964, 1533.
- 8 (a) M. Branca, B. Pispisa and C. Aurisicchio, *J. Chem. Soc., Dalton Trans.*, 1976, 1543; (b) M. G. B. Drew, J. Nelson, F. Esho, V. McKee and S. M. Nelson, *J. Chem. Soc., Dalton Trans.*, 1982, 1837; (c) V. McKee and S. S. Tandon, *ibid.*, 1991, 221; (d) X.-M. Chen, S. M. J. Aubin, Y.-L. Wu, Y.-S. Yang, T. C. W. Mak and D. N. Hendrickson, *J. Am. Chem. Soc.*, 1995, **117**, 9600.
- 9 E. Constable, S. M. Elder, J. Healy and D. A. Tocher, *J. Chem. Soc., Dalton Trans.*, 1990, 1669.
- 10 C. J. O'Connor, *Prog. Inorg. Chem.*, 1982, **29**, 203.
- 11 A. C. T. North, C. Phillips and F. S. Mathews, *Acta Crystallogr., Sect. A*, 1968, **24**, 351.
- 12 A. Altomare, M. C. Burla, M. Camalli, G. Cascarano, C. Giacovazzo, A. Guagliardi and G. Polidori, *J. Appl. Crystallogr.*, 1994, **27**, 435.
- 13 G. M. Sheldrick, SHELXTL, Release 5.03, Siemens Analytical X-ray Instruments Inc., Madison, WI, 1992.
- 14 W. Kraus and G. Nolze, POWDER CELL, Program for X-ray powder patterns calculation, Federal Institute for Materials Research and Test, Berlin, 1995.
- 15 (a) A. K. Powell and S. L. Heath, *Comments Inorg. Chem.*, 1994, **15**, 255; (b) N. N. Greenwood and A. Earnshaw, *Chemistry of the Elements*, Pergamon Press, Oxford, 1994, p. 1265.
- 16 A. G. Orpen, L. Brammer, F. H. Allen, O. Kennard, D. G. Watson and R. Taylor, *J. Chem. Soc., Dalton Trans.*, 1989, S1.
- 17 L. S. Dent Glasser, F. P. Glasser and H. F. W. Taylor, *Q. Rev. Chem. Soc.*, 1962, **16**, 343; A. Deschanvers and B. Raveau, *Rev. Chim. Miner.*, 1968, **5**, 201.

Received 22nd October 1997; Paper 7/07623A